

Content from this work may be used under the terms of the CC BY 3.0 licence (© 2019). Any distribution of this work must maintain attribution to the author(s), title of the work, publisher, and DOI

UPGRADE OF CERN'S PSB DIGITAL LOW-LEVEL RF SYSTEM

M. E. Angoletta[†], S. C. P. Albright, A. Findlay, M. Jaussi, J. C. Molendijk, N. Pittet
 CERN, Geneva, Switzerland

Abstract

The CERN PS Booster (PSB) is the first circular accelerator in the LHC proton injector chain. The upgrade of this four-ring machine is underway within the framework of the LHC Injectors Upgrade project. The existing digital Low-Level RF (LLRF) system will also be upgraded. This paper outlines the LLRF capabilities required, their implementation and the challenges involved. Results of tests carried out to prepare for the LLRF upgrade are given.

INTRODUCTION

The CERN Proton Synchrotron Booster (PSB) is the first circular accelerator in the LHC proton injector chain. This four-ring machine is being upgraded [1] as part of the Long Shutdown 2 (LS2) activities, under the LHC Injector Upgrade project [2]. The PSB will restart in 2020 with a new injection energy/scheme, extraction energy, Btrain and Finemet-based High-Level RF (HLRF) [3] systems.

Table 1 shows the main PSB parameters after LS2. Two extraction energies are foreseen: a) 1.4 GeV for operation with the radioactive ion beam facility ISOLDE, b) 2 GeV for CERN's Proton Synchrotron (PS). Cycle and acceleration lengths will remain of 1.2 s and 0.53 s, respectively.

Table 1: Post-LS2 Main PSB Parameters

	Energy	Revolution frequency
Injection	160 MeV	992 kHz
Extraction - a	1.4 GeV	1.748 MHz
Extraction - b	2 GeV	1.807 MHz

POST-LS2 LLRF SYSTEM

Hardware and Software

In 2014 we successfully deployed innovative digital Low-Level RF (LLRF) systems at the PSB restart [4]. They controlled the ferrite-based HLRF systems in each ring and a test Finemet HLRF in Ring 4 [5].

These five LLRF systems are now being upgraded to control the new Finemet-based HLRF systems [3]. The LLRF systems for PSB Rings 1 to 4 control the HLRF and the beam for their respective ring. A fifth one, called Ring 0 LLRF, controls the HLRF systems and beam in PSB Ring 4 for user-selectable cycles, replacing the standard Ring 4 LLRF. Its aim is to carry out dedicated Machine Development (MD) sessions via custom software and firmware.

Figure 1 shows the LLRF building blocks for one ring, their functions and input/output signals. Each LLRF system includes five motherboards instead of the three used before LS2. Each PSB ring comprises three HLRF systems located in sectors 5, 7 and 13, respectively. Each HLRF includes 12 Finemet cells and delivers 8 kV total voltage.

A single LLRF motherboard, shown as FMC-DSP Carrier C to E in Figure 1, controls the HLRF of a sector. Sixteen complete cavity voltage/phase servoloops are embedded in the FPGA and share one Analogue to Digital (ADC) input and one Digital to Analogue (DAC) output. The achievable bandwidth is nearly a factor of 10 higher than that previously obtained [5].

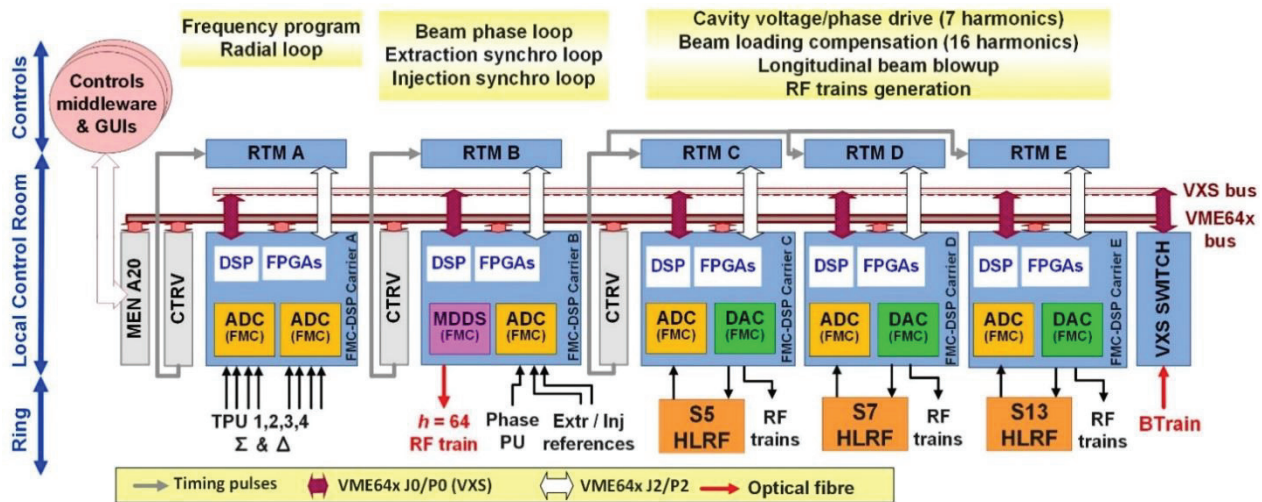


Figure 1: Post-LS2 LLRF for one PSB ring. Keys: MDDS – Master Direct Digital Synthesiser, ADC – Analogue-to-Digital Converter, DAC – Digital-to-Analogue Converter, TPU – Transverse Pick-Up, CTRV – Timing Receiver Module, MEN A20 – Master VME board, RTM – Rear Transition Module, DSP – Digital Signal Processor, FPGA – Field Programmable Gate Array, FMC – FPGA Mezzanine Card.

[†]maria.elena.angoletta@cern.ch

The information on the measured magnetic field is received from the new Btrain system over optical fibre [6].

The LLRF system is clocked by a fixed 122.7 MHz clock. This is now the standard for all machines equipped with the same LLRF and has been already deployed in the Extra Low ENergy Antiproton (ELENA) ring [7, 8] and in the Low Energy Ion Ring (LEIR) [9].

HLRF Impedance Effects on Beam Stability

The impedance of the Finemet HLRF will limit the longitudinal stability at high intensities and small emittances. Figure 2 shows the voltage induced at harmonics $h = 1$ to 20 on the Ring 4 test Finemet cavity by an 800 E10 proton beam, accelerated with the ferrite-based HLRF only.

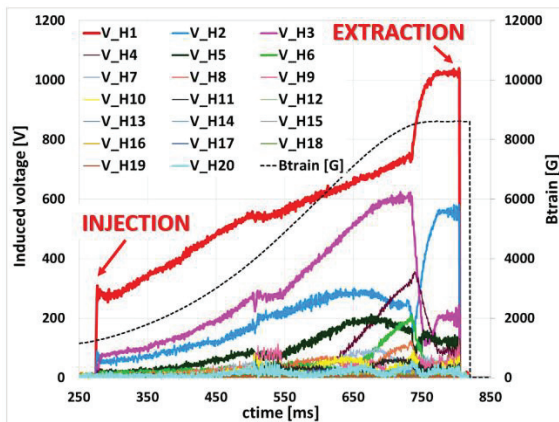


Figure 2: Voltage induced on the first 20 harmonics of the Ring 4 Finemet cavity by an 800 E10 proton beam.

Empirical microwave stability threshold calculations suggest that microwave instability is a significant limitation. Beam dynamics simulations [10] of longitudinal stability after LS2 included servoloops on HLRF at harmonics $h = 1$ to 8. These simulations have shown that current operational beams will be within the stable parameter space. The final stability margin should be better than the current prediction due to the higher number of planned servoloops.

HLRF System Operation

A distributed cavity concept is deployed that harnesses the wideband characteristics of the new HLRF systems. Specifically, the voltage required at a precise harmonic is distributed over the three HLRF systems in a ring. The LLRF controls them to drive/dampen the same harmonics; this saves precious RF voltage budget in beam loading compensation, for harmonics driven in a sector and not in others. Up to seven harmonics can be controlled in voltage/phase for operation and for MDs. In particular, harmonics $h = 1, 2, 3, m$ (where m is a high harmonic for longitudinal blowup [4]) are used for operational beams. Up to three additional harmonics can be available for MDs. The remaining harmonics damp the beam-induced field. The LLRF voltage set-point generation includes a computer-controlled scaling, that enables balancing the power amplifier drive in each sector. This accounts for partial HLRF availability due to faulty Finemet cells. The beam relative phasing of all harmonics is implemented through

programmable phase offsets, applied to the Multi-Harmonic Local Oscillator (MHLO) in each motherboard. This automatically rotates the phase of the demodulated cavity voltages of all harmonics, such that the imposed in-phase (real) set-point results in the desired RF field phase in each sector. The MHLO scales the azimuthal rotation of each harmonic to keep a constant bucket shape. An operationally viable method to measure the phase shift as a function of RF frequency was devised in 2018 [11].

The control/acquisition power chain is adjusted to allow sufficient regulation room even when the HLRF amplifier gain collapses near full power. Voltage set-point and cavity drive are limited as a function of frequency to not overdrive the HLRF. A gap relay short-circuits a HLRF system between cycles, when no voltage is requested. At the beginning of each cycle and before injecting the beam, we will carry out long-term measurements of HLRF MOSFET polarisation changes due to radiation.

Longitudinal Blowup Methods

The FPGA embedded servoloops implement also longitudinal blowup capabilities. Methods already validated with beam are available:

- Single-tone $n \cdot f_s$ phase modulation at a high harmonic, where f_s is the synchrotron frequency.
 - Playback of a phase noise file at the accelerating h .
- New methods will be deployed, such as:
- Single-tone $n \cdot f_s$ phase modulation on a subset of harmonics with the same phase excursion.
 - Single-tone $n \cdot f_s$ phase modulation through the MHLO. The phase excursion is scaled with the harmonic to provide a constant bucket shape.
 - Playback of a phase-noise file (up to 0.67 s long) on a subset of harmonics with the same phase excursion.
 - Playback of a phase-noise file through the MHLO. The phase excursion is scaled with the harmonic to allow constant bucket shape.

The detected cavity voltage is insensitive to the phase modulation as phase rotations are performed in closed-loop. The beam phase loop does not react to the blowup phase noise if the frequencies applied are high enough so as not to move the bunch barycentre. Below this threshold the system must use blowup phase data to estimate and compensate for bunch movements.

Interface to Other Systems

RF trains at $h = 1$ to 16 are generated on two DAC outputs of FMC-DSP Carrier boards D to E. The $h = 8$ train is sent to the tune measurement system. The $h = 1$ train is sent to the old PSB transverse damper system and to the tomoscope [12]. The LLRF to tomoscope interface will be upgraded to that deployed in ELENA: the tomoscope will receive accelerating harmonic number, accelerating and shaping detected voltages as well as Btrain and Btrain derivative values. The new PSB transverse damper [13] requires an $h = 64$ sweeping clock. The secondary MDDS channel will be used to directly synthesize this RF train. It will then be distributed over optical fibre.

MD RESULTS FOR POST-LS2 LLRF

We give here a selection of MD results, in view of post-LS2 operation. Previous results are also available [4, 5].

Five-board System Configuration

The post-LS2 configuration was validated in the Ring 0 LLRF. Five boards successfully co-operated to accelerate a $1.1E13$ protons/bunch beam by controlling the ferrite HLRF systems and eight harmonics in the Finemet HLRF.

Injection Synchronisation Process

Injection from Linac4 requires the synchronisation of the RF frequency on all PSB rings to carry out a bunch-to-bucket transfer including longitudinal painting. The injection synchronisation process, based on that previously deployed in ELENA [8], was achieved at energies of both 50 MeV (Linac2) and 160 MeV (Linac4). Figure 3 shows the process carried out at 160 MeV on the four PSB rings.

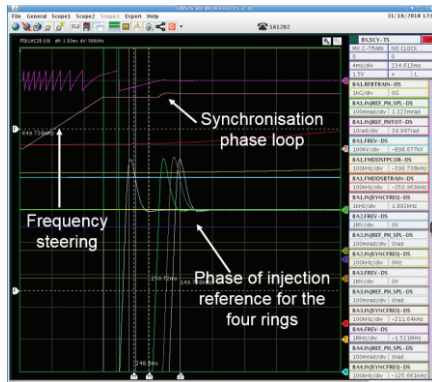


Figure 3: Injection synchronisation process at 160 MeV.

Longitudinal Blowup Reliability Run

In 2018 we did a successful reliability run of controlled longitudinal emittance blowup with RF phase noise [14]. We used low (80 E10 protons per ring, ppr), moderate (160 E10 ppr) and high (up to 500 E10 ppr) intensity cycles. The beam parameters were unchanged for operation with phase noise compared to standard longitudinal blowup by modulation at a high harmonic. Figure 4 shows the excellent particle distribution obtained at extraction with longitudinal blowup by phase noise for a low intensity, Bunch Compression Merging and Splitting (BCMS) LHC beam.

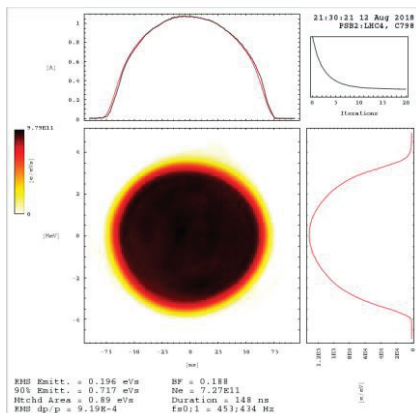


Figure 4: Particle distribution for a BCMS beam in 2018.

New Extraction Synchronisation Scheme

The synchronisation at extraction of split ($h = 2$) beams, previously carried out with respect to an $h = 2$ external reference signal, was upgraded to a synchronisation with an $h = 1$ reference. The method was based on that already successfully deployed in LEIR [9]. This new extraction synchronisation scheme allows choosing which of the two buckets is extracted first to the PS and simplifies the interface between the two machines.

Btrain Reliability Run

A reliability run for the post-LS2 Btrain measurement system [15] and corresponding White-Rabbit (WR) optical fibre distribution [6] took place in 2018. Starting from the existing ELENA [7] version, the PSB LLRF firmware was modified to integrate the latest WR core. This allowed fixing link failures on the client side in real-time and accessing advanced diagnostics such as the latency measurement of Btrain frames and the transmitted/received/lost frames count. A software switch selected the old, TTL or the new, WR Btrain as input to the frequency program calculation. Extensive logging facilities were implemented in the LLRF to validate the new Btrain data stream. The WR Btrain was successfully used for operational and for MD beams.

Finemet HLRF Reliability Run

Extended reliability runs and MD sessions were carried out with the Finemet HLRF system installed in PSB Ring 4 and controlled by the Ring 0 LLRF. The Finemet HLRF system replaced the ferrite one for acceleration at $h = 1$, $h = 2$ and longitudinal blowup. It was also used at $h = 3$ for triple harmonic capture and bunch shaping. Nominal beam parameters were achieved for operational beams. The combined LLRF-HLRF availability was of 99%, thus giving great confidence in the post-LS2 operation.

OUTLOOK AND CONCLUSIONS

The additional hardware required for the PSB LLRF systems upgrade is under production and will be available by January 2020. A LLRF test stand controlling a 6-cell Finemet HLRF will be installed in the HLRF laboratory by June 2019. It will allow validating the 16 servoloops implementation for a HLRF system. It will also provide advanced testing capabilities to the HLRF team.

LLRF and HLRF systems will be installed in the PSB by March 2020, to carry out the hardware commissioning. The PSB will take beam from September 2020 onwards; a detailed schedule of the required cycles already exists. The first beam will be extracted to the PS in December 2020.

The commissioning of the new LLRF capabilities will greatly profit from the MDs carried out before LS2 in the PSB and from the operational experience gained in other machines equipped with the same LLRF. Future PSB LLRF system evolution will also be inspired by achievements in other machines. An example is the bunch length measurement and monitoring over the cycle provided by the ObsBox [16] LLRF add-on, already planned for AD [17] and ELENA [8].

Content from this work may be used under the terms of the CC BY 3.0 licence (© 2019). Any distribution of this work must maintain attribution to the author(s), title of the work, publisher, and DOI

REFERENCES

- [1] K. Hanke *et al.*, “Status and Plans for the Upgrade of the CERN PS Booster”, in *Proc. IPAC '15*, Richmond, Virginia, US, May 2015, pp. 3905-3907.
- [2] M. Meddahi *et al.*, “LHC Injectors Upgrade Project: Towards New Territory Beam Parameters”, presented at IPAC'19, Melbourne, Australia, May 2019, paper THX-PLM1, this conference.
- [3] M. M. Paoluzzi *et al.*, “The New 1-18 MHz Wideband RF System for the CERN PS Booster”, presented at IPAC'19, Melbourne, Australia, May 2019, paper WEPRB107, this conference.
- [4] M. E. Angoletta *et al.*, “Operational Experience with the New Digital Low-Level RF System for CERN's PS Booster”, in *Proc. IPAC '17*, Copenhagen, Denmark, May 2017, pp. 4058-4061.
- [5] M. E. Angoletta *et al.*, “Control and Operation of a Wideband R System in CERN's PS Booster” in *Proc. IPAC '17*, Copenhagen, Denmark, May 2017, pp. 4050-4053.
- [6] P.P.M. Jansweijer, H.Z. Peek, E. de Wolf, “White Rabbit: Sub-nanosecond timing over Ethernet”, *Nuclear Instruments and Methods in Physics Research A* 725 (2013), pp. 187-190.
- [7] M.E. Angoletta *et al.*, “Initial Beam Results of CERN ELENA's Digital Low-Level RF System”, in *Proc. IPAC '17*, Copenhagen, Denmark, May 2017, pp. 4054 – 4057.
- [8] M. E. Angoletta, M. Jaussi, J. C. Molendijk, “The New Digital Low-Level RF System for CERN's Extra Low Energy Antiproton machine”, presented at IPAC'19, Melbourne, Australia, May 2019, paper THPRB069, this conference.
- [9] M. E. Angoletta *et al.*, “The new LEIR Digital Low-Level RF system”, in *Proc. IPAC '17*, Copenhagen, Denmark, May 2017, pp. 4062-4065.
- [10] D. Quartullo, S. Albright, E. Shaposhnikova, “Studies of Longitudinal Beam Stability in CERN PS Booster After Upgrade”, in *Proc. IPAC '17*, Copenhagen, Denmark, May 2017, pp. 4469-4472.
- [11] S. Albright, “Beam-based Measurements of Relative RF Phase”, presented at IPAC'19, Melbourne, Australia, May 2019, paper THPRB066, this conference.
- [12] <http://tomograp.home.cern.ch>
- [13] G. P. Di Giovanni *et al.*, “Commissioning of a New Digital Transverse Damper System at the PSB”, presented at IPAC'19, Melbourne, Australia, May 2019, paper MOPTS085, this conference.
- [14] S. Albright, “Time Varying RF Phase Noise for Longitudinal Emittance Blow-up”, presented at IPAC'19, Melbourne, Australia, May 2019, paper THPRB067, this conference.
- [15] C. Grech, A. Beaumont, M. Buzio, N. Sammut, J. Vella Wallbank, “Performance Evaluation of Real-Time Synchrotron Magnetic Measurement systems”, submitted for publication.
- [16] M. Ojeda *et al.*, “Processing High-Bandwidth Bunch-by-Bunch Observation Data from the RF and Transverse Damper Systems of the LHC”, in *Proc. ICAPEPCS2015*, Melbourne, Australia, October 2015, pp. 841-844.
- [17] M. E. Angoletta, S. Albright, M. Jaussi, V. R. Myklebust, J. C. Molendijk, “New Low-Level RF and Longitudinal Diagnostics for CERN's AD”, presented at IPAC'19, Melbourne, Australia, May 2019, paper THPRB070, this conference.